

The Role of Structure Directing Agents on Chemical Switching Properties of Nanostructured Conducting Polyaniline (NSPANI)

Deepshikha¹ and *T. Basu²¹Amity Institute of Biotechnology, Amity University, Noida-201303, Uttar Pradesh, INDIA²Amity Institute of Nanotechnology, Amity University, Noida-201303, Uttar Pradesh, INDIAAvailable online at: www.isca.in(Received 14th July 2011, revised 24th July 2011, accepted 3rd August 2011)

Abstract

The nanostructured conducting polyanilines was synthesized using single and composite structure directing agents such as sodium dodecyl sulphate, sodium dodecyl benzene sulphonate, camphor sulphonic acid by chemical method. The effects of nature and concentration of structure directing agents (both single and composite) on pH characteristics, redox behaviour and solvent pattern were investigated using UV-Vis spectroscopy, Transmission electron microscopy, Cyclic voltammetry and Dynamic light scattering. Both concentration and nature of structure directing agents could influence the pH behaviour and workable pH range. The transition from conducting state to insulating state of all nanostructured conducting polyanilines occurred at higher pH than bulk PANI. The Transmission electron microscopy and Dynamic light scattering results showed that the morphology and the dimension of nanostructured conducting polyanilines at the doped and undoped state depended on the nature of structure directing agents used for polymerization. The redox properties were independent of nature and concentration of structure directing agents but electrochemical activity and solution behaviour of nanostructured conducting polyanilines depended on the nature of structure directing agents.

Keywords: Polyaniline, nanostructure, doping, undoping, dedoping, electrochemical activity.

Introduction

Nanostructured conducting polymers (NSCPs) have received considerable attention as compared to bulk conducting polymers due to their high surface-to-volume ratio¹, electron transfer rate², surface free energy³ and electrical conductivity^{4,5}. They also provide interesting functional properties such as short path lengths for the transport of ions, improved cycle life of an electrode due to better accommodation of the strain caused by electrochemical reaction^{6,7} mixed conductive mechanism of both electronic and ionic conductivity, which lowers the interfacial impedance between electrodes and electrolyte and light weight and large ratio of specific discharge power to weight. The nanostructured conducting polyaniline (NSPANI) is unique among the family of conducting polymers because of its ease of synthesis, environmental stability, tunable electronic conductivity, versatile electrochemical switching behavior⁸, reversible doping/dedoping chemistry⁹⁻¹¹, excellent mechanical strength, suitability for making composites with different types of binders, which make it as one of the most suitable component in the fabrication of macromolecular electronic devices such as opto and microelectronics, photonics¹², sensors in chemical¹³, electrochemical^{14,15} and biological applications¹⁶.

PANI is a phenylene-based polymer having –NH– group on either side of the phenylene ring. The oxidation and reduction takes place on this –NH– group, and various forms are obtained due to the number of imine and amine segments on the PANI chain. Thus it can exhibit unique electrochemical switching property that is its electrical

properties can be reversibly controlled by both charge-transfer doping and protonation. This unique phenomenon has made polyaniline versatile for various applications such as sensors, opto and microelectronic devices. The ability of PANI to exhibit a number of intrinsic oxidation states has also been utilized in the inhibition of corrosion of metals. The emeraldine base has been applied as an active component in light-emitting devices. The ability of PANI to undergo reversible oxidation and reduction has also resulted in its utilization as electrode materials for rechargeable batteries and capacitors. It is possible to replace metallic conductors and semi-conductors with the use of PANI in many applications such as transistors, switches, electrochemical actuators, lithographic resists, lightning protection, microelectronics, solar cells, circuit boards, polymer electrolytes, heating elements, electrostatic discharge (ESD) and electromagnetic interference shielding (EMI) applications¹⁷. The solution behavior of NSPANI makes totally new product ideas possible. These include electroactive inks, paints, coatings, adhesives, electrochromic “smart” windows, electrically conductive transparent films and conductive high performance fibres.

NSPANI with different morphologies have been synthesized using various techniques such as template synthesis, self-assembly, emulsions and interfacial polymerization¹⁸⁻²¹, seeding polymerization²², rapidly mixed reaction²³ and surfactant-directing methods^{24,25}. One of the most elegant and facile way of synthesizing NSPANI is use of structure directing agent (SDA) which can act as a soft template. The SDA controls the polymerization in a restricted zone so that the crystal

growth can take place in a definite manner. It has been proposed that at low temperature, the liquid crystal-like arrays formed between the inorganic-cluster and the self-assembly of organic structure directing agent (SDA) i.e. the amphiphilic molecule, readily undergo reversible lyotropic transformations leading to nano structured materials²⁶.

We have synthesized NSPANI using single and composite structure directing agents²⁷. It has been reported that the chemical nature, concentration and combination of SDA have profound influence on the nano dimension as well as electronic property of NSPANI. However, to our knowledge, there are no detailed reports on the study of effect of nature and concentration of SDA on doping/undoping behavior, redox chemistry and solubility of NSPANI. It is absolutely necessary to investigate the above properties of NSPANI in detail to explore its full spectrum of application. In this manuscript, attempts have been made to study the influence of nature and concentration of SDA on the pH, redox and solubility pattern of various NSPANI, synthesized using different formulation, using UV-Vis spectroscopy, Cyclic voltammetry (CV), Dynamic light scattering (DLS) and Transmission electron microscopy(TEM).

Material and Methods

Aniline (Sigma-Aldrich), sodium dodecyl sulphate (SDS) (Qualigen), ammonium persulfate $(\text{NH}_4)_2\text{S}_2\text{O}_8$ (E-Merck), sodium dodecyl benzene sulfonate (SDBS) (Sigma-Aldrich) and camphor sulphonic acid (CSA) (Qualigen), sodium hydroxide and phenylhydrazine were purchased from Aldrich. Hydrochloric acid (Qualigen), N-methyl-2-pyrrolidone (NMP) (Sigma-Aldrich), dimethyl sulphoxide (DMSO) (Sigma-Aldrich), N,N-dimethyl-formamide (DMF) (Sigma-Aldrich) were used in the present experiment. Deionized water from a Millipore-MilliQ was used in all cases to prepare aqueous solutions. Monomer was double distilled before polymerization.

Polymerization procedure: The NSPANI was synthesized using single and composite structure directing agents according to a previously communicated procedure²⁷. The structure directing agents include sodium dodecyl sulphate (SDS), dodecyl benzene sulphonate (SDBS) and camphor sulphonic acid (CSA). Table 1 represents the synthesis condition of NSPANI using various concentrations of SDS, SDBS and CSA. In a typical synthesis, aniline (0.02 M) was first dissolved into a dilute aqueous solution (0.02 M) of acid (HCl or CSA). The aniline solution was added to an aqueous solution of SDA under stirring condition. The mixture was then placed in the low temperature bath, so that the temperature was maintained at 0^o to 5^oC. An aqueous solution of the oxidizing agent, $(\text{NH}_4)_2\text{S}_2\text{O}_8$, in ice-cold water was added to the above mixture. The polymerization was allowed to proceed for 3 to 4 h with stirring. After that the stirring was stopped and the mixture was allowed to age under static condition for 1-3 days at 277–278^oK for complete

polymerization. The colloidal solution was precipitated using acetone. The precipitate was washed with deionized water to remove unreacted chemicals. The polymer powder was dried under vacuum at 60^oC.

Table-1
Formulation of nanostructured conducting polyaniline (NSPANI) synthesis

Sample Code	Aniline: SDS	Aniline: $(\text{NH}_4)_2\text{S}_2\text{O}_8$	Aniline: HCl	Aniline : CSA
S1	1:1	1:0.5	1:1	-
S2	1:2	1:1	1:1	-
S3	1:3	1:1.5	1:1	-
S4	1:4	1:2	1:1	-
D1	1:1	1:1	1000:1	-
D2	1:2	1:1.5	500:1	-
D3	1:3	1:1.5	333:1	-
SC1	1:1	1:1	1:0.5	1:1
SC2	1:2	1:1	1:1	1:1
SC3	1:3	1:1	1:1.5	1:1
SC4	1:4	1:2	1:2	1:2
DC1	1:2	1:0.5	1:1	1:1
DC2	1:3	1:1.5	1:1	1:1

Instrumentation: The UV-Vis absorption spectra were measured using a Shimadzu UV-1800 UV-Vis spectrophotometer. Morphological imaging was obtained by Transmission electron microscope (TEM), using a JEOL JEM-1011 at 80 kV and Dynamic light scattering (DLS) measurements were performed using a Malvern 4800 Autosizer employing a 7132 digital correlator. Cyclic voltammetric study was carried out using Autolab Potentiostat/Galvanostat Model 273A.

Results and Discussion

Effect of concentration of structure directing agents (SDA) on the pH switching behavior of NSPANI: The UV-Vis spectra of various all NSPANI show three characteristic absorption bands at 320–380, 400–432 and 790-856 nm wavelength (spectra not shown)²⁷. The first absorption band is related to π - π^* band transition, second and third absorption bands are due to the formation of polaron and bipolaron respectively²⁸. A gradual bathochromic shift of the polaron absorption band in the visible region has been observed with increase in the concentration of SDA²⁷. The red shift is attributed to the nanostructure, extended π conjugation and increased conductivity.²⁹

When dark green colour of NSPANI (S1, S2, S3 and S4) dispersions have been treated with 0.1 M NaOH dropwise, the colour of nano dispersions change from green to violet. Upon base treatment, the polaron absorption band at 790-832 nm has shifted to 568-575 nm which is assigned to the exciton band of the EB form and the polaron band in the UV region disappears due to removal of charge at the undoped state²⁹. The violet colour of nanodispersion signifies complete conversion of emeraldine salt (ES) to emeraldine base (EB) which is the undoped condition of polyaniline (scheme 1).

Table-2
Effect of pH on nanostructured conducting polyaniline (S1,S2,S3and S4) and bulk polyaniline

Name of sample	Colour at the undoped State	^a Wavelength (nm)	^b Wavelength (nm)	Workable pH range	^c Bandgap (eV)	^d Bandgap (ev)
S1	Violet	785	569	2.24-9.78	1.58	2.18
S2	Violet	796	570	3.35-10.33	1.56	2.18
S3	Violet	811	575	3.53-12.96	1.53	2.16
S4	Violet	832	568	3.57-13.03	1.49	2.18
Bulk Polyaniline	Violet		-	1.91-7.53	-	-

a=Wave length of visible region polaron absorption at the doped state; b=Wave length of visible region polaron absorption at the undoped state; c= Band gap energy(E) in the doped state(eV),d=Band gap energy(E)in the undoped state(eV); $E=hc/\lambda$

Table-3
Effect of pH on nanostructured conducting polyaniline (D1,D2 and D3)

Name of sample	Colour at undoped state	Workable pH range	^a Wavelength (nm)	^b Wavelength (nm)	^c Bandgap (eV)	^d Bandgap (eV)
D1	Dark blue	3.96-10.04	842	575	1.476	2.161
D2	Dark blue	2.33-13.13	855	594	1.453	2.092
D3	Dark blue	3.73-10.08	855	584	1.453	2.128

a=Wave length of visible region polaron absorption at the doped state; b=Wave length of visible region polaron absorption at the undoped state; c= Band gap energy (E) in the doped state (eV); d=Band gap energy(E)in the undoped state(eV); $E=hc/\lambda$

Table-4
Effect of pH on nanostructured conducting polyaniline (SC1,SC2,SC3,DC1,DC2)

Name of sample	Colour at undoped state	Workable pH range	^a Wavelength (nm)	^b Wavelength (nm)	^c Bandgap (eV)	^d Bandgap (eV)
SC1	Blue	3.76-9.05	804	520	1.546	2.211
SC2	Blue	3.84-9.84	870	530	1.428	2.132
SC3	Blue	2.28-12.57	818	552	1.519	2.252
DC1	Dark blue	3.94-9.96	824	570	1.508	2.180
DC2	Dark blue	2.37-13.16	792	573	1.569	2.169

a=Wave length of visible region polaron absorption at the doped state; b=Wave length of visible region polaron absorption at the undoped state ; c= Band gap energy(E) in the doped state(eV) d=Band gap energy(E)in the undoped state(eV); $E=hc/\lambda$

Table-5
DLS results of the best nanostructured conducting polyaniline during pH switching

Sample name	^a Z-Average (d-nm)	^b Z-Average (d-nm)	^c Polydispersity index(PDI)	Increase in dimesion (%)	^d Z-Average (d-nm)	^e Polydispersity index(PDI)
S4	49.14	61.95	0.351	26	53.06	0.322
D2	20.91	45.85	0.263	119	24.25	0.346
SC3	491.8	540	0.469	10	503	0.415
DC2	230.9	410	0.742	60	360	0.695

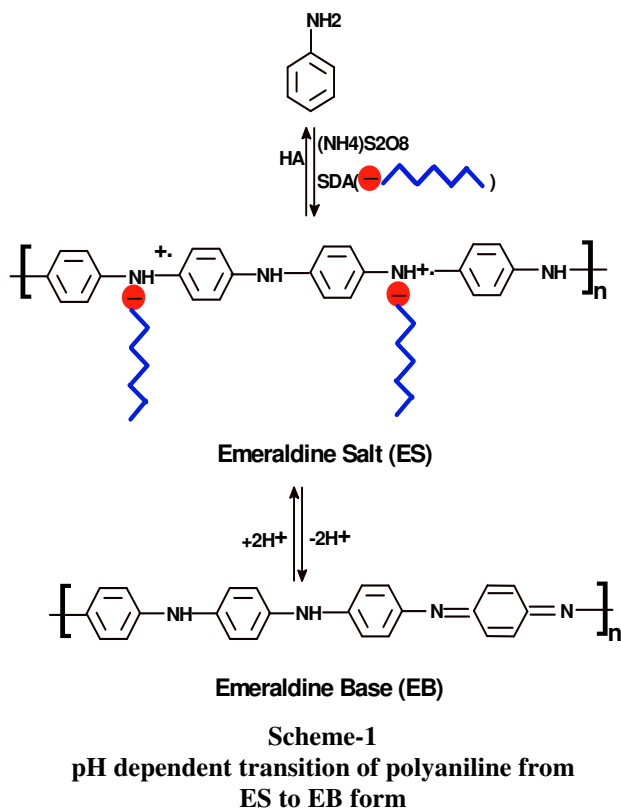
a= Z-Average(d-nm) of doped NSPANI; b= Z-Average(d-nm) of undoped NSPANI

c= Polydispersity index(PDI) of undoped NSPANI

d= Z-Average(d-nm) of dedoped NSPANI

e= Polydispersity index(PDI) dedoped NSPANI

As no discrete change has been identified in the absorption maxima of π - π^* band on undoping so we have focused our study only on polaron absorption band in the visible region because polaron band is more localized. Table 2 represents pH behavior of NSPANI(S1, S2, S3 and S4) when SDS is used as a single SDA. It has been observed that undoping of S4 is difficult and occurs at high pH as compared to S1,S2, S3 indicating the difficulty of undoping S4.



Further HOMO and LUMO band gaps at the doped and undoped state are calculated using the formula $E=hc/\lambda$ where h = Planck's constant (6.63×10^{-34} J-s), c = velocity of light (3×10^8 m/s), λ = wavelength of absorption (nm). Interestingly, the band gaps of NSPANI are much lower than the bulk PANI (2 eV at the doped form) confirming the nano dimension^{30,34}. At the undoped state, band gap is increased when conducting ES of NSPANI is converted into insulating EB form (Table 1). All NSPANI (S1, S2, S3 and S4.) have almost identical band gaps at the undoped state irrespective of the amount of the SDS used for polymerization. However, the workable pH range increases with increase in SDS concentration for example workable pH range for S4 has been found to be as 3.57-13.03. Interestingly, the conversion from conducting to insulating state of all S1, S2, S3 and S4 occurs at much higher pH than bulk PANI (1.91-7.53). S4 is considered to be the best sample.

Upon base treatment of NSPANI (D1, D2 and D3), blackish green color of nano dispersions convert to blue color dispersion indicating undoping of NSPANI(D1, D2 and D3). The exciton band of EB form of NSPANI nano dispersions has been found to be in the range of 575-594 nm (table 3). It has been observed that D2 is difficult to be

undoped as compared to D1 and D3 as its exciton band appears at 594 nm at pH of 13.13 (table 3). This is due to the highly ordered nanostructure and extended π -conjugation of D2²⁷. Furthermore, the workable pH range of D2 is wider and band gap between HOMO and LUMO at the undoped state is minimum as compared to D1 and D3. In case of complex SDA system, on undoping of NSPANI with base solution, the polaron absorption band at 804-870 nm transforms to exciton band of the EB form with an absorption maxima at 520 to 573 nm (figure not shown). Table 4 represents the pH behaviour of NSPANI (SC1, SC2, SC3, DC1 and DC2).

With increase in concentration of SDS for (SC1, SC2 and SC3), the absorption maxima of exciton band exhibits a bathochromic shift. As SC3 and DC2 provide maximum workable pH range and minimum band gap energy between HOMO and LUMO at the undoped state, SC3 and DC2 are considered to be the best samples in their respective series. In fact, the trend is similar to SDS or SDBS alone as SDA.

Effect of nature of SDA on the pH switching characteristics of NSPANI dispersion: From the above discussion, a comparison of pH switching characteristics is drawn between S4, D2, SC3, DC2 in order to study the effect of nature of SDA. Figure 1 shows the UV-Visible spectra of NSPANI. The UV-Visible spectra (Figure 1) reflect that the visible region polaron absorption band at the doped state and exciton band at the undoped state of NSPANI dispersion occur at higher wavelength when SDBS is used as one of the SDA. In fact, when SDBS is used as SDA, complete undoping is difficult which is assigned to the strong complex forming ability of SDBS with the positively charged polymer backbone. Introduction of CSA with either SDS or SDBS does not change the basic pH behaviour. Workable pH range is independent of the nature of SDA, it depends on the concentration of SDA. It has been also observed, on dedoping all of these NSPANI regain their conductive state immediately and this process can be repeated in number of times.

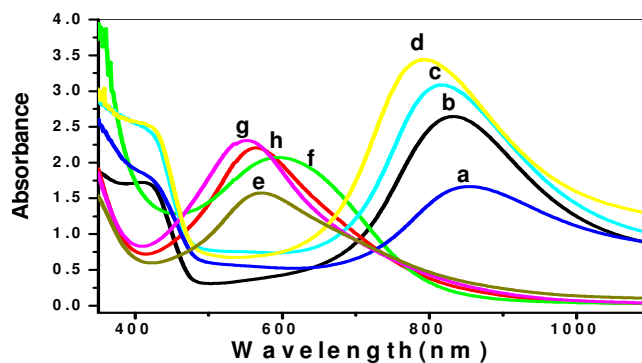
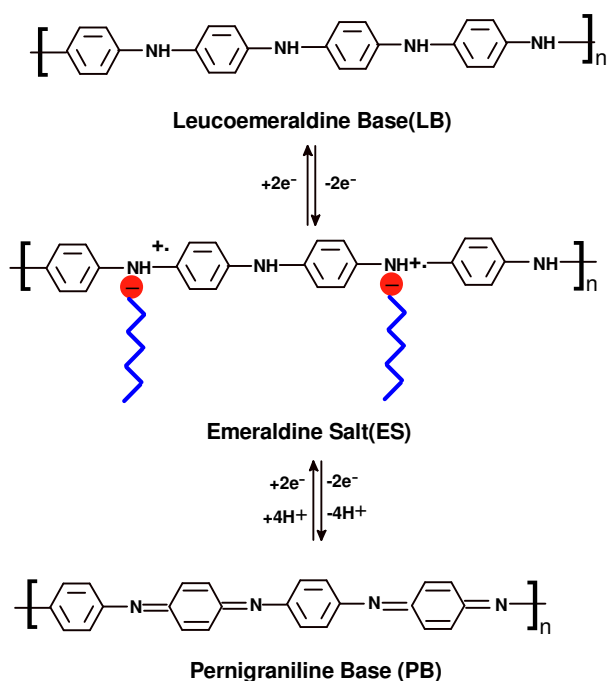


Figure-1
UV-Vis spectra of nanostructured conducting polyaniline (a) D2(doped); (b) S4(doped); (c) SC3(doped); (d) DC2(doped); (e) S4(undoped); (f) D2(undoped); (g) SC3 (dedoped); (h) DC2(dedoped)

Effect of concentration of structure directing agent on the redox behavior of NSPANI: NSPANI shows remarkable reversible redox switching properties. Addition of oxidizing agent like 0.07 M APS to a dispersion of NSPANI at the ES form (dark green) causes rapid oxidation to produce the violet color for NSPANI (S1, S2, S3, S4, SC1, SC2, SC3) and blue colour for NSPANI (D1, D2, D3, DC1, DC2) of pernigraniline base (PB) dispersion resulting deprotonation. Upon oxidation, a band at 560-585 appears, characteristic of the PB form of polyaniline, while the peaks of the original ES disappear (Data not shown).

This behavior is independent of the SDA concentration but depends on type of SDA used. When SDBS is used as SDA, PB shows blue color irrespective of the nature of dopant acid, i.e HCl or CSA and the corresponding HOMO and LUMO band gap is comparatively lower (2.1 eV). The reduction behavior of the NSPANI nano dispersion treated with aqueous (4 M) phenylhydrazine has been studied using UV-Vis spectroscopy. After 10 min, reduction to the fully reduced leucoemeraldine base (LB) form has been almost completed, as evidenced by the disappearance of ES band and the appearance of a strong characteristic $\pi-\pi^*$ band at 423-430 nm. However, the reduction behavior of NSPANI is also independent of the concentration as well as type of SDA. All of these NSPANI dispersions show unique reversibility in terms redox switching behavior. In PB and LB form of NSPANI, it converts to complete insulating form due to complete undoping (scheme 2). At the LB form, NSPANI has lower band gap (around 2.9 eV) than the bulk PANI (4 eV)³⁰ indicating nano dimension.



Scheme-2
The redox mechanism of polyaniline

On the basis of pH behavior, redox properties, and the values of band energy gap it is clear that S4, D2, SC3 and DC2 are the best samples. So these four samples have been investigated in residual part of our investigation.

Dynamic Light Scattering studies: It is well known that the contraction and expansion take place in conducting polymers due to the ion movement into and out of conducting polymers which also changes their flexibility and leads to their potential use as actuators as well as piezoelectric transducers^{31,32}. At the doped stage, the conducting polymers are rigid and possess smaller size where as at the undoped stage they show good flexibility and enhanced dimension. Table 5 summarizes the DLS results of various undoped and dedoped NSPANI. DLS reflects the hydrodynamic volume of the particle. The DLS studies reflect that on undoping the hydrodynamic volume of all NSPANI increases resulting in an increase in flexibility in the polymer chain which can cause an enhancement in swelling in the dispersion. It is found that nature of the SDA strongly influences the flexibility and dimension of NSPANI at the undoped stage. The increase in dimension for S4 is 26 % where as D2 undergoes 119 % increase in dimension on undoping. Reattachment of SDA to NSPANI, i.e., on dedoping with acid brings the dispersion into the conducting state and regains their dimension. The dedoped samples have almost identical size to the doped samples for S4 and D2. The high extensibility and reversibility of D2 on undoping reveal its potential as an actuator and piezoelectric transducer. Polydispersity index (PDI) value of all the nano dispersion is remained almost unchanged at the undoped state except for DC2 while PDI increases dramatically. The recovery of DC2 to its original dimension is the lowest (12%) indicating degradation of polymer on undoping.

Transmission electron microscopy (TEM) : Figure 2 shows TEM (transmission electron micrographs) images of the samples. The TEM of undoped and dedoped of emeraldine salt (ES) nano particles increase and lie in the range of 20-46 nm for D2 and S4 whereas in case of doped samples the sizes are in the range of 20-32 nm for S4 and 10-28 nm for D2. (TEM image not shown)²⁷. It has been observed that on undoping of S4, the large cluster like structures are formed due to the inherent aggregation tendency of S4 while in case of D2 though the undoping causes an increase in dimension but the segregated spherical morphology of D2 is still maintained as shown in TEM image Figure 2(c). This shows that D2 nano particles are evenly dispersed and they have less tendency to get aggregated both at doped and undoped state. Due to reversible chemical switching properties of PANI, on dedoping the EB form can convert back to ES state and TEM image shows that NSPANI (both S4 and D2) regain their dimension with fairly narrow size distribution of 20 -35 nm. In case of D2 the distinct individual nanoparticles with spherical morphology are seen Figure 2(d) while S4 on dedoping, exhibits spherical nano particulate morphology with somewhat aggregated form.

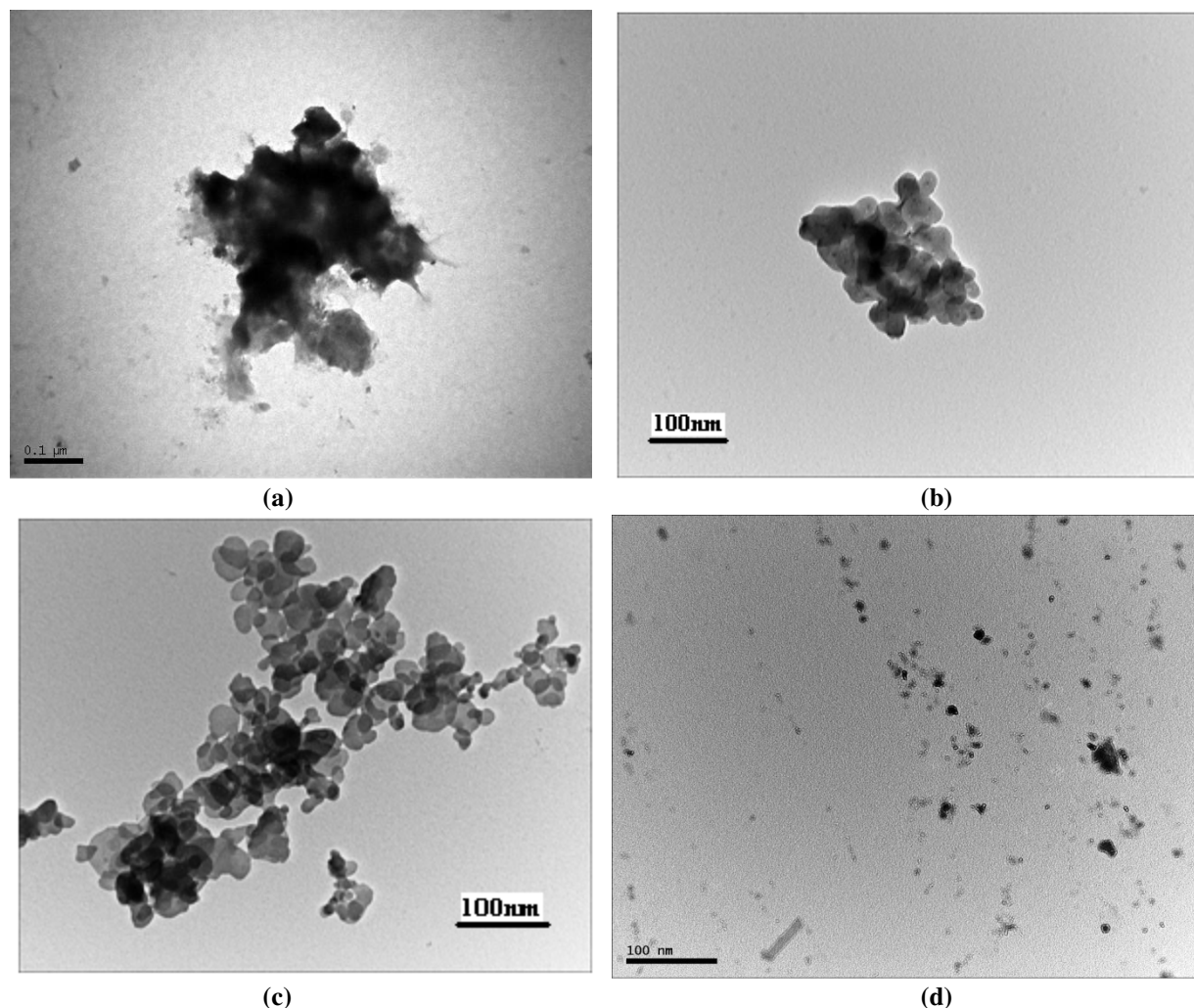


Figure-2
TEM images of (a) S4(Undoped) b) S4(Dedoped) (c) D2(Undoped) (d) D2(Dedoped)

Effect of nature of SDA on Electrochemical properties of NSPANI dispersion: Figure 3 shows cyclic voltammograms (CV) of S4, D2, SC3 and DC2. The potential was swept from - 500 mV to + 1100 mV (vs. Ag/AgCl), as polyaniline is redox active within this region at acidic pH. The CV shows the characteristics peaks of PANI³³⁻³⁵ such as peaks a and b corresponding to the transformation of leucoemeraldine base (LB) to emeraldine salt(ES) and ES to pernigraniline salt (PS), respectively. On the reverse scan, peaks b' and a' correspond to the conversion of PS to ES and ES to LB, respectively. S4 converts from LB to ES form at much lower potential (136 mV) and from ES to PS at higher potential (735 mV) than SC3 indicating its higher electroactivity. So, in this case on introduction of CSA retards the electroactivity of NSPANI as supported by pH behaviour whereas the introduction of CSA does not affect the electrochemical behavior of NSPANI dispersion to a great extent when SDBS is one of the SDA. While comparing CV of S4 and D2, it is found that the peak potential for the conversion of LB to ES and ES to PS shifts towards much lower potential in case of D2 as compared to S4 and D2 shows almost reversible redox transformation for the conversion of LB to ES state indicating its efficacy towards electro chemical activity.

All of these NSPANI show electrochemical switching property for number of times without losing the electroactivity and S4 and D2 are found to be the best of all indicating their suitability for rechargeable battery and OLED application³⁶⁻³⁸. S4 shows the slowest and diffused kinetics as compared to other NSPANI as shown in the current vs time plot for CV studies (Figure 4) which may be due to the presence of a small redox peak associated with the formation of p-benzoquinone and hydroquinone as a side product and its somewhat aggregated structure. Both D2 and DC2 offer much higher anodic and cathodic peak current than S4 and SC3 indicating higher electro catalytic activity.

Effect of nature of SDA on the solubility pattern of SDA: The solubility of NSPANI was investigated by dissolving 2 mg of NSPANI powder samples in 10 ml of solvents such as NMP, DMSO, DMF, acetone, methanol, toluene and benzene. The solution was filtered and weight of the precipitate was taken after drying at 60^oC under vacuum to find out the percent solubility. The clear solution was investigated through UV-Visible spectroscopy.

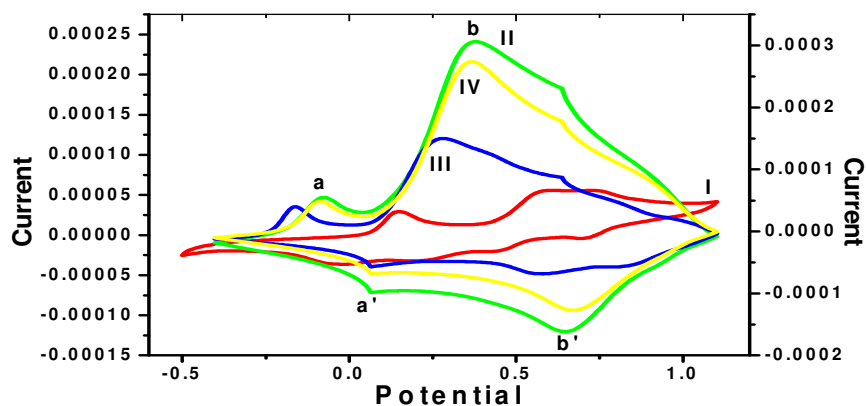


Figure-3

Cyclic Voltammogram of nanostructured conducting polyaniline (I) S4; (II) D2;(III) SC3; (IV) DC2

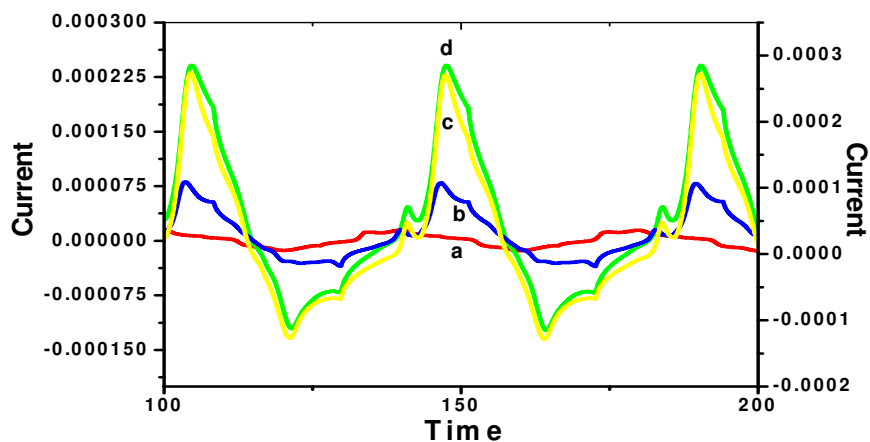


Figure-4

Current vs Time plot of nanostructured conducting polyaniline(a) S4;(b) D2;(c) SC3;(d) DC2

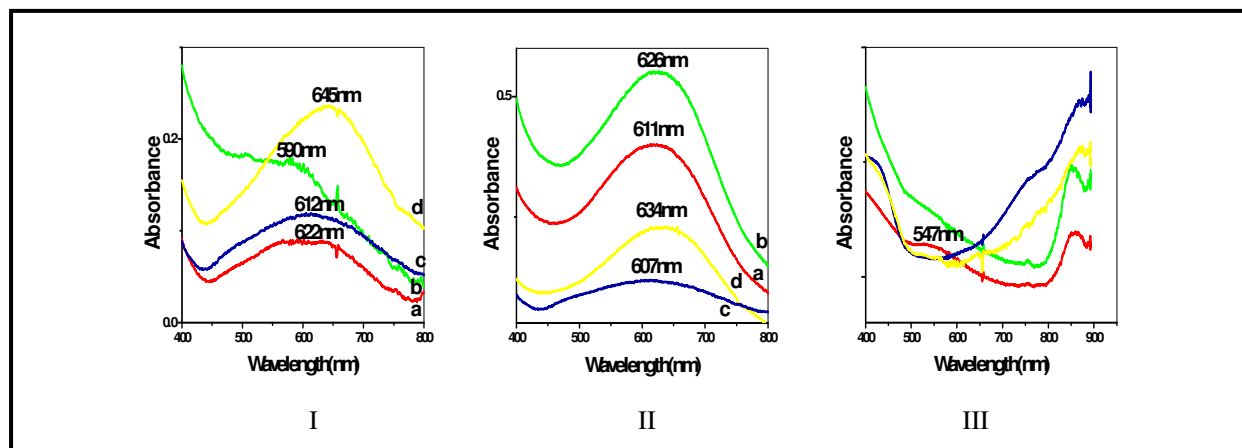


Figure-5

UV-Vis spectra of nanostructured conducting polyaniline after treating with (I) NMP;(II)DMSO;(III) DMF (a=S4,b=D2,c=SC3,d=DC2)

N-Methyl pyrrolidone(NMP): N-Methyl-2-Pyrrolidone (NMP) is a powerful, aprotic solvent with high solvency and low volatility. The solution of NSPANI (S4, D2, SC3 and DC2) is blue in colour and all NSPANI powders are completely soluble in the NMP as shown in Figure 5(I) and table 6). UV-Vis spectroscopy shows hypsochromic shift (590nm-645nm) for the polaron bands. Maximum

blue shift occurs for D2 (590nm). This is due to the strong interaction between basic polar solvent (NMP) and D2. The blue colour of the solution indicates undoping of the NSPANI samples and NMP is acting as a base as per the reaction 1.



Table-6
Solubility pattern NSPANI powder in different organic solvents

S.No.	Name of sample	Solubility in different organic solvents							
		NMP	DMSO	DMF	Methanol	Chloroform	Acetone	Toluene	Xylene
1	S4	●	●	■	■	○	○	○	○
2	D2	●	●	■	■	○	☆	○	○
3	SC3	●	●	○	○	○	○	○	○
4	DC2	●	●	○	○	○	○	○	○

●= completely soluble; ○= Insoluble; ■= partially soluble; ☆= Sparingly soluble

Dimethyl sulphoxide (DMSO): DMSO is an important polar aprotic solvent. When NSPANI powders are dissolved in DMSO, the colour of solution becomes blue (table 6). NSPANI shows 100% solubility and get undoped in DMSO as shown in Figure 5(II). S4 shows maximum blue shift (611nm) indicating comparatively stronger interaction with DMSO as compared to other NSPANI.

Dimethyl formamide (DMF): When the solubility of NSPANI powder has been checked with DMF (table 6), only S4 and D2 show partial solubility in DMF without undoping where as SC3 and DC2 are completely insoluble in DMF figure 5(III).

Other solvents: The solubility of NSPANI is also checked in other solvents such as methanol, acetone etc and the results are tabulated in table 6. D2 is sparingly soluble in acetone. All of them are insoluble in toluene and xylene due to the impossibility of the non polar solvent to dissolve both the hydrophilic dopant part and the hydrophobic organic part of the polymer.

Conclusion

The nature of SDA profoundly monitor pH switching behavior, redox characteristics and solvent pattern of NSPANI. It is observed that NSPANI dispersion is difficult to be undoped and the conversion from conducting state to insulating state occurs at higher pH than bulk PANI. The concentration as well as the nature of SDA monitor the pH characteristics of NSPANI dispersion. With increase in concentration of SDA workable pH range increases. When SDBS is used as SDA, strong complex is formed with positively charged polymer backbone. It has been found that D2 is the most difficult sample to be undoped and exhibits lowest HOMO and LUMO band gap at the doped and undoped state. Introduction of CSA in place of HCl, decreases workable pH range, retards electrochemical activity and complex forming ability when SDS is one of the SDA. All of NSPANI undergo expansion in dimension on undoping and dedoping can recover their

original dimension. This reversibility also depends on the type of SDA. The TEM results show that S4 has a tendency to agglomerate both at the doped and undoped state where as D2 prefers to be remained as a discrete particle even at the undoped state indicating its efficacy as SDA. The redox behavior is independent of concentration as well as nature of SDA but the electrochemical properties and solubility pattern depend on the nature of SDA. The solvent which can act as a base and cause undoping of the NSPANI, is the best solvent such as NMP.

Acknowledgement

We acknowledge the financial assistance received from the Department of Biotechnology, Govt. of India (Project No BTPR 11123/MD/32/41/2008 DBT) for the financial support, India. We are thankful to Dr. A.K. Chauhan (Founder President, Amity University, Uttar Pradesh) for providing the platform of research at Amity University Uttar Pradesh and we also offer our sincere thanks to Dr (Mrs) Balvider Shukla Director General A.S.E.T, Dr. R. P. Singh, Director, AINT, Prof. A. K. Srivastava, Director General, AIB, AUUP for their constant support and encouragement. We are also thankful to Dr. Jasbir Singh and Dr. Baljeet Kaur, ICAR New Delhi for conducting TEM study.

References

1. Pruna A., Branzoi V. and Branzoi F., Application of template-based polyaniline nanotubes synthesized in anodic porous alumina, *Rev. Roum. Chim.*, (55) 293-298 (2010)
2. Luo X., Morrin A., Killard A.J. and Smyth M.R., Application of nanoparticles in electrochemical sensors and biosensors, *Electroanalysis*, (18), 319 (2006)

3. Malhotra B.D., Chaubey A. and Singh S.P., Prospects of conducting polymers in biosensors, *Anal. Chim. Acta*, (578), 59 (2006)
4. Wu C.G. and Bein T., Conducting Polyaniline Filaments in a Mesoporous Channel Host, *Science*, (264), 1757-1759 (1994)
5. Yin Z.H., Long Y.Z., Gu C.Z., Wan M.X. and Duvail J.L., Current-Voltage... Nanotube, and CdS Nanorope, *Nanoscale Res. Lett.*, (4), 63-69 (2009)
6. Pei Q.B. and Inganas O., Electrochemical applications of the bending beam method 1. mass transport and volume changes in polypyrrole during redox, *J Phys. Chem.* (96), 10507-10514 (1992)
7. Pei Q.B. and Inganas O., Electrochemical applications of the bending beam method electroshrinking and slow relaxation in polypyrrole, *J. Phys. Chem.*, (97), 6034-6041 (1993)
8. Xia L., Wei Z. and Wan M., Conducting polymer nanostructures and their application in biosensors, *J. of Colloid and Interface Science*, (341), 1-11(2010)
9. Huang W.S., Humphrey B.D. and MacDiarmid A.G., Polyaniline, a novel conducting polymer: Morphology and chemistry of its oxidation and reduction in aqueous electrolytes, *J. Chem. Soc.*, (82), 2385-2400 (1986)
10. MacDiarmid A.G., Chiang J.C., Halpern M., Huang W S., Mu S.L., Somasiri N.L.D., Wu W. Q. and Yaniger S.I., Polyaniline: interconversion of metallic and insulating forms, *Mol. Cryst., Liq. Cryst.*(121), 173-180 (1985)
11. MacDiarmid A.G., Application of Electroactive Polymers, *Synth. Met.*, (84), 27-34 (1997)
12. Holdcroft S., Patterning p-conjugated polymers. *Adv. Mater.*, (13), 1753 (2001)
13. Virji S., Huang J., Kaner R.B. and Weiller B.H. Polyaniline Nanofiber Gas Sensors: Examination of Response Mechanisms, *Nano Lett.*, (4), 491(2004)
14. Janata J. and Josowicz M., Conducting polymers in electronic chemical sensors, *Nature Mater.*, (2), 19 (2003)
15. Wang J., Chan S., Carlson R.R., Luo Y., Ge G.L., Ries R.S., Heath J.R., and Tseng H.R., Electrochemically fabricated polyaniline nanoframework electrode junctions that function as resistive sensors, *Nano Lett.*, (4), 1693 (2004)
16. Liu J., Tian S. and Knoll W., Properties of Polyaniline/Carbon Nanotube Multilayer Films in Neutral Solution and Their Application for Stable Low-Potential Detection of Reduced beta-Nicotinamide Adenine Dinucleotide, *Langmuir.*, (21), 5596 (2005)
17. Palaniappan S. and John A. Polyaniline materials by emulsion polymerization pathway, *Prog. Polym. Sci.*, (33), 732-758 (2008)
18. Gupta V. and Miura N. Electrochemically deposited polyaniline nanowire's network, *Electrochemical and solid state letters*, (8), A630-A632 (2005)
19. Qiu H., Wan M., Matthews B. and Dai L. Conducting polyani-line nanotubes by template-free polymerization, *Macromol*, (34), 675 (2001)
20. Wei Z. and Wan M., Hollow microspheres of polyaniline synthesized with an aniline emulsion template, *Adv. Mater*, (14), 1314 (2002)
21. Huang J. and Kaner R.B., A General Chemical Route to Polyaniline Nanofibers, *J. Am. Chem. Soc.*, (126), 851(2004)
22. Xing S., Zhao C., Jing S. and Wang Z., Morphology and conductivity of polyaniline nanofibers prepared by 'seeding' polymerization. *Polymer* (47) 2305-2313 (2006)
23. Li D. and Kaner R., Shape and aggregation control of nanoparticles: not shaken, not stirred, *J Am Chem Soc.*, (128), 968-975 (2006)
24. Li G. and Zhang Z., Synthesis of dendritic polyaniline nanofibers in a surfactant gel, *Macromolecules*, (37), 2683-2685 (2004)
25. Kuczynska A., Uygun A., Kaim A., Wachnik H W, Yavuz A G and Aldissi M Effects of surfactants on the characteristics and biosensing properties of polyaniline. *Polym Int.* (59),1650-1659 (2010)
26. Kresge C.T., Leonowicz Roth W.J., Vartuli J.C. and Beck J.S., Ordered mesoporous molecular sieves synthesized by a liquid-crystal template mechanism, *Nature*, (359), 710 (1992)
27. Deepshikha and Basu T., Synthesis and Characterization of Nanostructured Conducting Polyaniline using various Structure Directing Agents, *J. of experimental Nanoscience*, (in press) (2011)
28. Stejskal J. and Kratochvil P., Polyaniline Dispersions 2 UV-V is Absorption, Spectra, *Synth. Met.*, (61), 225 (1993)
29. Moulton S.E., Innis P.C., Kane-Maguire L.A.P., Ngamna O., and Wallace G.G., Polymerisation and characterisation of conducting polyaniline nanoparticle dispersions, *Current Applied Physics*, (4), 402-406 (2004)

30. Hassan P. A., Sawant S. N., Bagkar N.C., and Yakhmi J.V. Polyaniline Nanoparticles Prepared in Rodlike Micelles, *Langmuir* (20), 4874-4880 (2004)
31. Madden P.G.A., Development and modeling of conducting polymer actuators and the fabrication of a conducting polymer based feedback loop, Dissertation, Massachusetts Institute of Technology (2003)
32. Sahoo H, Pavoov T and Vancheeswaran S., Actuators based on electroactive polymers. *Current Science*, (81), 10 (2001)
33. Han M.G., Cho S.K., Oh S.G. and Im SS, Preparation and characterization of polyaniline nanoparticles synthesized from DBSA micellar solution. *Synth. Met.* (126), 53 (2002)
34. Morrin A., Guzman A., Killard A.J., Pingarron J.M. and Smyth M.R., Characterisation of horseradish peroxidase immobilised on an electrochemical biosensor by colorimetric and amperometric techniques, *Biosens Bioelectron*, (18), 715 (2003)
35. Wallace G.G., Spinks G.M., Kane-Maguire L.A.P. and Teasdale P.R., *Conductive Electroactive Polymers: Intelligent materials systems* (2nd. ed), CRC Press, London, 237 (2003)
36. Karami H., Mousavi M.F. and Shamsipur M.A. new design for dry polyaniline rechargeable batteries, *J. of Power Sources*, (117), 255-259 (2003)
37. Benvenho A.R.V., Serbena J.P.M., Lessmann R. and Hummelgen I.A., Efficient Organic Light-Emitting Diodes with Fluorine-Doped Tin-Oxide Anode and Electrochemically Synthesized Sulfonated Polyaniline as Hole Transport Layer, *Brazilian Journal of Physics*, (35), 1016-1019 (2005)
38. Hebner T.R., Wu C.C., Marcy D., Lu M.H. and Sturm J.C., Ink-jet printing of doped polymers for organic light emitting devices, *Applied Physics Letters*, (72), 519-521(1998)